metals

MDPI

Article

High-Strength Behavior of the $Al_{0.3}CoCrFeNi$ High-Entropy Alloy Single Crystals

Irina V. Kireeva *, Yuriy I. Chumlyakov, Zinaida V. Pobedennaya, Anna V. Vyrodova and Anastasia A. Saraeva

National Research Tomsk State University, Siberian Physical Technical Institute, 634050 Tomsk, Russia; chum@phys.tsu.ru (Y.I.C.); pobedennaya_zina@mail.ru (Z.V.P.); wirodowa@mail.ru (A.V.V.); anastasia16-05@yandex.ru (A.A.S.)

* Correspondence: kireeva@spti.tsu.ru; Tel.: +7-960-972-11-75

Received: 29 July 2020; Accepted: 16 August 2020; Published: 26 August 2020

Abstract: The main disadvantage of fcc (face-centred cubic lattice) high-entropy alloys is the low stress level at the yield point ($\sigma_{0.1}$) at a test temperature above room temperature. This restricts their practical application at high test temperatures from 773 K to 973 K. In this study, we found that a high stress level was reached at the yield point $\sigma_{0.1} \approx$ G/100–G/160 (G is the shear modulus) of the [001]- and $[\bar{1}44]$-oriented crystals of the $Co_{23.36}Cr_{23.29}Fe_{23.80}Ni_{21.88}Al_{7.67}$ ($Al_{0.3}CoCrFeNi$) high-entropy alloy (HEA) within a wide temperature range of 77–973 K under tension, due to the occurrence, of nanotwins, multipoles, dislocations under plastic deformation at 77 K and the subsequent precipitation of ordered $L1_2$ and B2 particles. It was shown that grain boundaries are not formed and the samples remain in a single-crystal state after low-temperature deformation and subsequent ageing at 893 K for 50 h. Achieving a high-strength state in the $Al_{0.3}CoCrFeNi$ HEA single crystals induces the orientation dependence of the critical resolved shear stresses (τ_{cr}) at T ≥ 200 K ($\tau_{cr}[\bar{1}44] > \tau_{cr}[001]$), which is absent in the initial single-phase crystals, weakens the temperature dependence of $\sigma_{0.1}$ above 573 K, and reduces plasticity to 5–13% in the $[\bar{1}44]$ orientation and 15–20% in the [001] orientation.

Keywords: $Al_{0.3}CoCrFeNi$ high-entropy alloy; single crystals; high-strength state; $L1_2$ and B2 particles; twinning

1. Introduction

High-entropy alloys (HEAs) are a new class of alloys that have a combination of unique properties, namely, high strain hardening, good plasticity and good ductile fracture strength [1–6]. At low temperatures, single-phase fcc (face-centred cubic lattice) HEAs are only comparable to high-strength materials ($\sigma_{0.1}$~G/140–G/220; here G is the HEA shear modulus, equal to 85, 81 and 67 GPa, respectively, at 77, 296 and 773 K [7]), which include materials with a yield point $\sigma_{0.1}$~G/100, and they are low-strength ($\sigma_{0.1}$ > G/360) at T ≥ 296 K, due to the strong temperature dependence of the yield point $\sigma_{0.1}$(T) [2–6]. Commonly, a high level of $\sigma_{0.1}$ in single-phase polycrystals is achieved by a decrease in grain size. However, in fine-grained HEA polycrystals, within the high-temperature range at T > 673 K, the $\sigma_{0.1}$ sharply decreases as a result of grain-boundary sliding (GBS) [2].

The fcc $Al_{0.3}CoCrFeNi$ alloy is one representative of the HEAs, which is characterized by medium stacking fault energy γ_0 = 0.051 J/m^2 and demonstrates a unique combination of properties, such as high strength, work hardening, good plasticity in tension at room and cryogenic temperatures, corrosion resistance, high oxidation resistance and excellent fatigue resistance [5,8–14].

The high level of strength properties at the yield point, achieved in the $Al_{0.3}CoCrFeNi$ HEA due to Al alloying in the single-phase state, led to the development of twinning at T < 296 K. In poly- and single crystals of the $Al_{0.3}CoCrFeNi$ HEA, twinning when interacting with slip provides a strong strain

hardening, and at the same time retains plasticity up to 30–70% [5,10]. In addition, the $Al_{0.3}$CoCrFeNi HEA is a precipitation-hardening alloy, and ordered $L1_2$ and B2 particles precipitate in it, which leads to an increase in the strength properties of this HEA [15–18]. Thus, with the precipitation of B2 particles, the tensile strength can be increased from 1200 MPa at room temperature to 1600 MPa at 77 K, while maintaining ductility up to 17% [10]. Despite this combination of unique properties at T < 300 K, the $Al_{0.3}$CoCrFeNi HEA in the high temperature range at T > 300 K, like other fcc HEAs, remains low-strength [1–5]. This impedes its practical application at high test temperatures from 773 K to 973 K.

In the present paper, in relation to $Al_{0.3}$CoCrFeNi HEA single crystals, an attempt has been made for the first time to achieve high stresses at the yield point $\sigma_{0.1}$, within the wide temperature range of 77–973 K, under tension, due to the occurrence of nanotwins, multipoles and dislocations under plastic deformation at 77 K, and the subsequent precipitation of ordered $L1_2$ and B2 particles. For this purpose, two orientations, $[\bar{1}44]$ and [001], were chosen for the following reasons. Firstly, in the $[\bar{1}44]$-oriented crystals, the maximum Schmid factor for twinning, $m_{tw} = 0.5$, is greater than the Schmid factor for slip, $m_{sl} = 0.4$, and these crystals are favorable for obtaining a dislocation structure with twins [19,20]. To obtain a dislocation structure without twins, [001]-oriented crystals were chosen in which, conversely, the Schmid factor for slip, $m_{sl} = 0.41$, is larger than the Schmid factor for twinning, $m_{tw} = 0.23$ [5]. Secondly, in the chosen orientations, the m_{sl} during deformation remains constant, due to the shear multiplicity in [001]-oriented crystals, which do not change during the precession in the $[\bar{1}44]$-oriented crystals [21]. This will allow the critical resolved shear stresses (CRSS) τ_{cr} of deformed crystals to be determined, provided that the single-crystal matrix is preserved after thermomechanical processing, due to plastic deformation at 77 K and subsequent ageing at 893 K for 50 h.

2. Materials and Methods

Single crystals of the $Co_{23.36}Cr_{23.29}Fe_{23.80}Ni_{21.88}Al_{7.67}$ ($Al_{0.3}$CoCrFeNi) (at.%) HEA were grown via the Bridgman method in a helium atmosphere using ingots cast in a resistance furnace (InterSELT, St.-Petersburg, Russia). To achieve a homogeneous distribution of the elements in the bulk of the ingots, they were remelted three times. The dog-bone-shaped tension samples had a gauge length of 12 mm and a cross section of 2×1.5 mm^2. The samples were cut using wire electrical discharge machining. The damaged surface layer was ground off mechanically, and then electrically polished in 200 mL of an H_3PO_4 + 50 g CrO_3 (phosphoric acid with chromium trioxide) electrolyte at room temperature. The crystals were homogenized in a helium atmosphere at 1473 K for 48 h, and then quenched in water. Homogenization leads to a uniform distribution of elements over the crystal volume, which, as will be shown below, is confirmed by the precipitation of $L1_2$ and B2 particles in the defect structure of the samples. To determine the orientation of the crystals, the diffractometric method was used by means of a DRON-3M X-ray diffractometer (Bourevestnik, St.-Petersburg, Russia) with monochromatic Fe Kα radiation, the technique for which was presented in [22]. The high-strength state $\sigma_{0.1} \approx$ G/100–G/120 was achieved in two steps. The first step consisted of the low-temperature plastic deformation at 77 K of the [001]-and $[\bar{1}44]$-oriented crystals, within which a stress level of 700 MPa ≈ G/120 was achieved in both orientations. This stress level was reached at a strain of 50% in the $[\bar{1}44]$-oriented crystals and at strain of 20% in the [001]-oriented crystals. The second step consisted of the ageing at 893 K for 50 h in a helium atmosphere of the deformed crystals, followed by cooling in water. During the selected ageing process, firstly, ordered $L1_2$ and B2 particles were precipitated, which contributed to an increase in stresses of $\sigma_{0.1}$ [15–17]. Secondly, the temperature of ageing, 893 K, was not sufficient for the recrystallization of the dislocation structure [2,15,17], which allows the samples to be preserved following deformation in a single-crystalline state. The mechanical properties within a temperature range of 77 to 973 K were determined using an Instron 5969 universal testing machine (Instron, Nowood, MA, USA) at a strain rate of 4×10^{-4} s^{-1}. For the test at 77 K, the sample and grips were immersed in a special vessel with liquid nitrogen, in which both were held for 10 min before the start of the test, and then the sample was deformed in liquid nitrogen. Tests in the temperature range of 200 to 973 K were carried out in a special heat chamber, which is included in the equipment of the Instron 5969 universal

testing machine. The heating/cooling rate of the chamber was 2 K/min. The sample was inserted in grips, heated/cooled together with the chamber, kept at each temperature for 30 min before testing, and then deformed. The CRSS values for slip were calculated using the expression $\tau_{cr} = \sigma_{0.1} \times m_{sl}$ (where $\sigma_{0.1}$ is the uniaxial stress at the 0.1% offset strain yield point). Transmission electron microscopy (TEM) studies were performed using a JEOL-2010 electron microscope (JEOL, Tokyo, Japan) at an accelerating voltage of 200 kV. The thin foils were prepared using double-jet electropolishing (TenuPol-5, "Struers", Ballerup, Denmark) with an electrolyte containing 20% sulphuric acid in methyl alcohol at room temperature, with 12.5 V applied voltage. The chemical composition of the single crystals after quenching was determined using the X-ray fluorescence method, by means of a wave-dispersive X-ray fluorescence XRF-1800 spectrometer (SHIMADZU, Kyoto, Japan), giving the atomistic percentages Co = 23.36%, Cr = 23.29%, Fe = 23.80%, Ni = 21.88% and Al = 7.67% (at.%). After quenching, the single crystals formed an fcc-based substitution solid solution, and did not contain dispersed particles of the second phase.

3. Results and Discussion

TEM investigations have shown that a planar dislocation structure, with dislocation pile ups, developed in the quenched $Al_{0.3}CoCrFeNi$ HEA single crystals after undergoing strain at 77 K [5]. In the [001]-oriented crystals, after undergoing strain of 20%, a high density of dislocations and multipoles was observed, but there were no twins. Thin twins with a thickness of 15–25 nm were found in the $[\bar{1}44]$-oriented crystals after undergoing strain of 50% at 77 K, simultaneously with a high density of dislocations and multipoles. Figures 1 and 2 display the dislocation structures after ageing at 893 K for 50 h of the deformed [001]- and $[\bar{1}44]$-oriented crystals of the $Al_{0.3}CoCrFeNi$ HEA, having undergone up to 20% and 50% strain, respectively, at 77 K.

During the ageing of the deformed crystals at 893 K for 50 h, recrystallization did not occur, grain boundaries were not detected and, therefore, the single-crystalline matrix was retained, as in samples deformed at 77 K (Figures 1 and 2). In the deformed $[\bar{1}44]$- and [001]-oriented crystals, ageing at 893 K for 50 h led to the precipitation of coherent $L1_2$ and non-coherent B2 particles [15,17]. In the diffraction pattern, clear super-structural reflections from $L1_2$ and B_2 particles were detected (Figures 1a and 2c). The particles differed in size d ($L1_2$ with d = 5–7 nm [17] and B2 with d = 30–40 nm (Figures 1c and 2b). The simultaneous precipitation of $L1_2$ and B2 particles in the matrix apparently suppressed the formation of the nuclei of grain boundaries, and the recrystallization process did not occur during this ageing, which requires further research and is not discussed in this paper. In polycrystalline $Al_{0.3}CoCrFeNi$ HEA, particles were precipitated in the grain body, $L1_2$, and at the grain boundaries, B2 [15]. In the initial quenched $Al_{0.3}CoCrFeNi$ HEA single crystals, when aged for 50 h at 893 K, only $L1_2$ particles with the same size were precipitated, while B_2 particles were not precipitated, due to the very high nucleation barrier, as a result of the need to generate large elastic and fcc/B2 interphase energies [17,18]. In the deformed $[\bar{1}44]$- and [001]-oriented crystals during ageing at 893 K for 50 h, $L1_2$ particles were distributed uniformly in the matrix, as was shown earlier in [17]. The precipitation of B2 particles occurred along the boundaries of multipoles and at dislocations, as well as near the twin boundaries in the deformed $[\bar{1}44]$-oriented crystals (Figures 1 and 2). Therefore, we can infer that not only grain boundaries in polycrystals, but also dislocations, multipoles and twins in deformed crystals facilitate the nucleation of B2 particles in an imperfect structure.

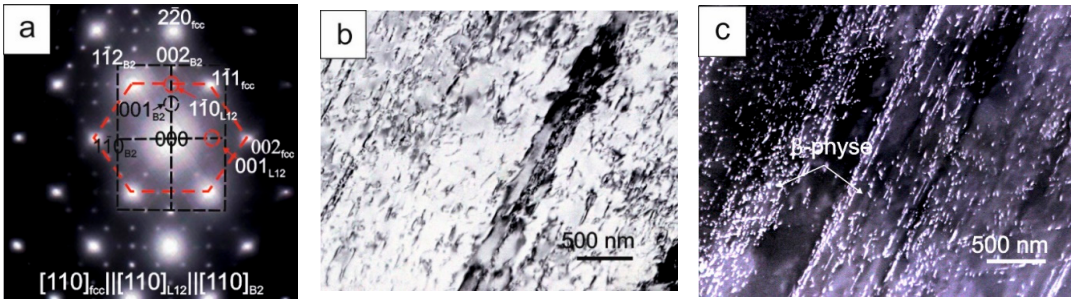

Figure 1. Dislocation structure of the [001] $Al_{0.3}CoCrFeNi$ HEA single crystals, deformed up to 20% strain at 77 K and aged at 893 K for 50 h: (**a**) diffraction pattern, showing super-structural reflections from $L1_2$ and B_2 particles; (**b**) the bright-field image, showing multipoles and high dislocation density; (**c**) the corresponding dark-field image of B_2 particles distributed along the boundaries of multipoles and at dislocations.

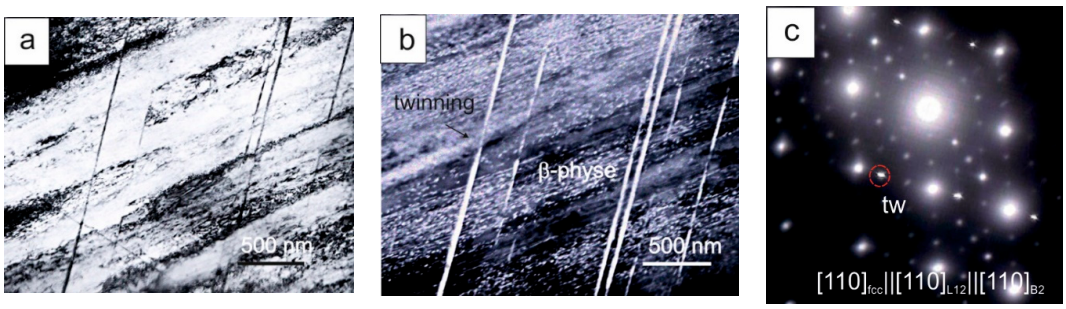

Figure 2. Dislocation structure of the $[\bar{1}44]$ $Al_{0.3}CoCrFeNi$ HEA single crystals, deformed up to 50% strain at 77 K and aged at 893 K for 50 h: (**a**) the bright-field image, showing twinning, multipoles and high dislocation density; (**b**) the corresponding dark-field image of B_2 particles distributed near twins, along the boundaries of multipoles and at dislocations; (**c**) diffraction pattern showing reflections from twins, $L1_2$ and B_2 particles.

Figure 3 shows the "stress–strain" ($\sigma(\varepsilon)$) curves at 77 K for the $[\bar{1}44]$- and [001]-oriented crystals, and indicates the level of strain at which the stress of 700 MPa was achieved during deformation. Figure 4 displays the temperature dependence of the yield point $\sigma_{0.1}$(T) and CRSS τ_{cr}(T) for three states (quenched, deformed and deformed + aged) of the $[\bar{1}44]$- and [001]-oriented crystals of $Al_{0.3}CoCrFeNi$ HEA, under tensile strain and within the wide temperature range T = 77–973 K.

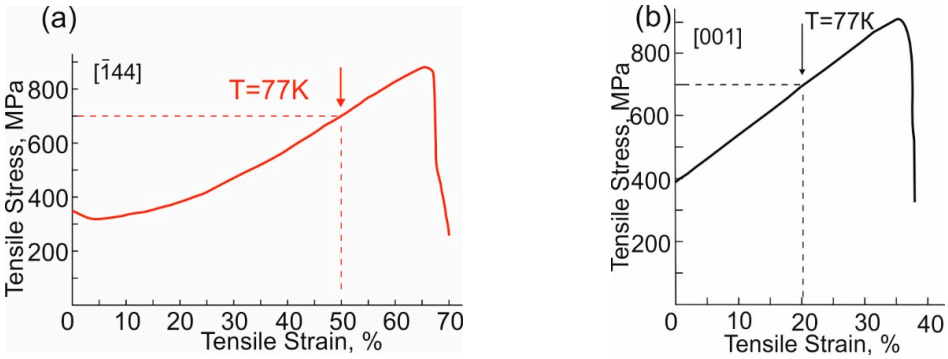

Figure 3. The stress–strain response in the quenched $[\bar{1}44]$- and [001]-oriented crystals of the $Al_{0.3}CoCrFeNi$ high-entropy alloy under tensile strain at 77 K; (**a**) $[\bar{1}44]$ orientation; (**b**) [001] orientation. The dotted line on the curve shows at what level of tensile strain the stress level of 700 MPa was reached in the studied orientations.The stress-strain response of the [001]-oriented crystals shown earlier in [5] (with permission from Elsevier, 2020) is given in this figure to demonstrate the orientation dependence of the mechanical behavior of the studied crystals under tensile strain.

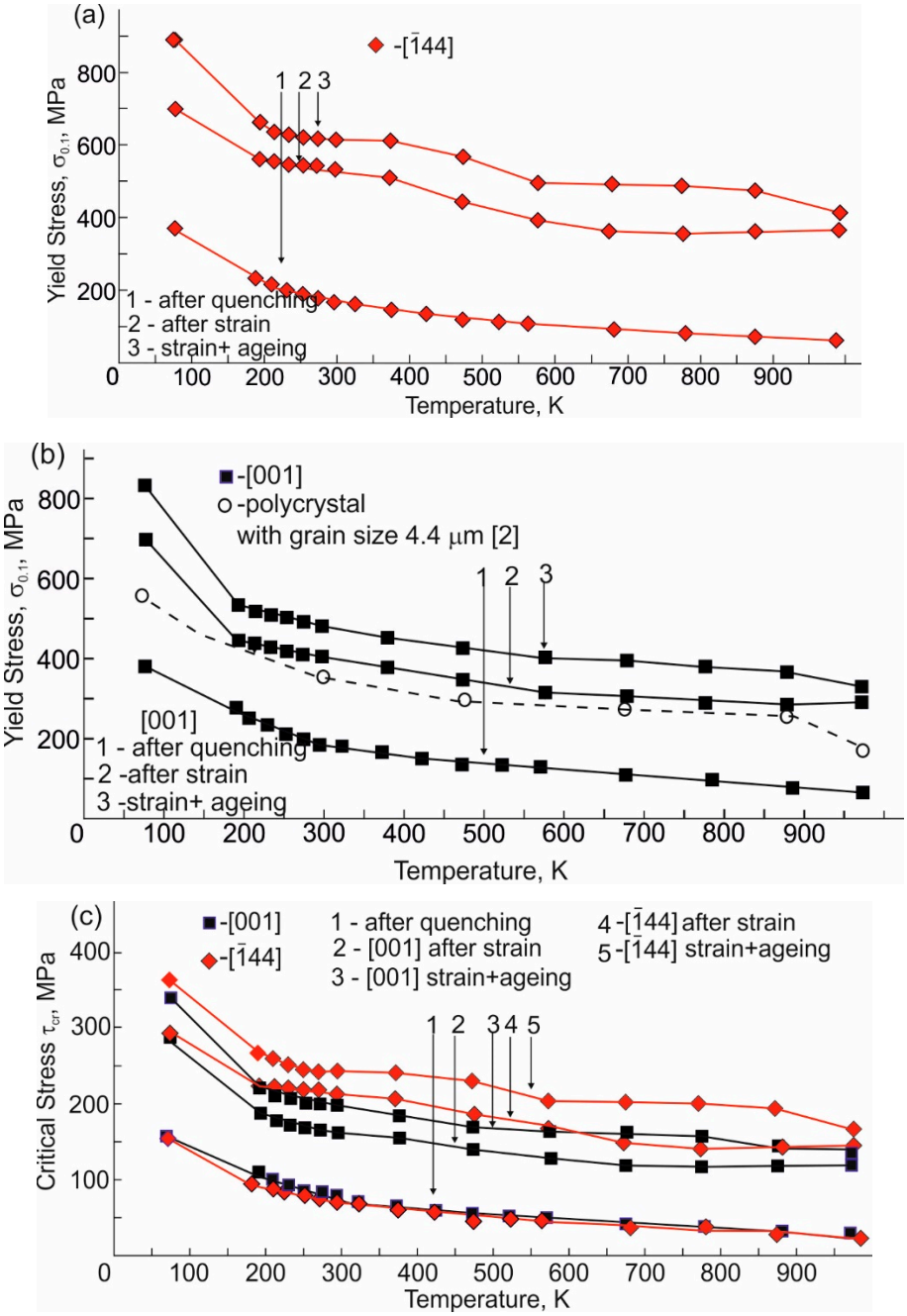

Figure 4. (**a**,**b**) Temperature dependence of yield point and (**c**) critical resolved shear stresses of the $Al_{0.3}$CoCrFeNi HEA single crystals under tensile strain. The temperature dependences of the yield point and critical resolved shear stresses of the quenched [001]-oriented crystals shown earlier in [5] (with permission from Elsevier, 2020) are given in this figure to demonstrate the absence of the orientation dependence of the critical resolved shear stresses in the quenched $Al_{0.3}$CoCrFeNi HEA single crystals under tensile strain.

It can be seen that after low-temperature deformation at 77 K, the $\sigma_{0.1}$ of the [1̄44]- and [001]-oriented crystals increased relative to the initial crystals in the studied temperature range; by 320 MPa at 77 K and 200–330 MPa at T ≥ 296 K. The precipitation of $L1_2$ and B2 particles additionally increased $\sigma_{0.1}$ by 130 and 200 MPa at 77 K, and by 80–130 MPa at T ≥ 296 K, relative to the deformed [001]- and [1̄44]-oriented crystals, respectively (Figure 4a,b). As a result, in the [1̄44]- and [001]-oriented crystals, $\sigma_{0.1} \approx$ G/100–G/160 within a temperature range of 77–973 K, due to joint hardening with a

dislocation structure and ordered particles (Figure 4a,b). Thus, $Al_{0.3}$CoCrFeNi HEA single crystals became high-strength at T < 296 K, and close to high-strength at T ≥ 296 K. In this state, as shown in Figure 5, $Al_{0.3}$CoCrFeNi HEA single crystals remained plastic.

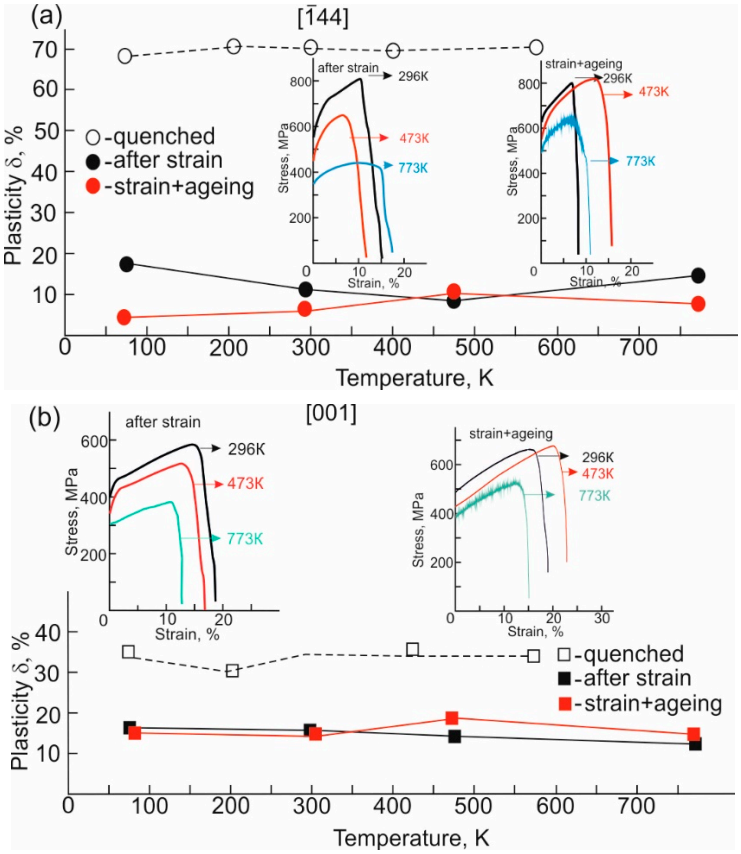

Figure 5. Plasticity in the $Al_{0.3}$CoCrFeNi HEA single crystals: (**a**) [1̄44] orientation; (**b**) [001] orientation. Plasticity of the quenched [001]-oriented crystals was taken from [5] (with permission from Elsevier, 2020).

In the initial quenched [1̄44]- and [001]-oriented crystals of the $Al_{0.3}$CoCrFeNi HEA, the τ_{cr} values were found to be independent of the crystal orientation within the studied temperature range, and the Schmid law was satisfied (Figure 4c, curve 1) [5,17]. The temperature dependence of the τ_{cr}(T) of both orientations consists of two sections, characteristic of the slip deformation of fcc substitution alloys [5,23]. At T < 373 K, there is a strong temperature dependence of τ_{cr}(T) (the thermally activated τ_S component of τ_{cr}), associated with the thermally-activated interaction of dislocations with substitution atoms. At T > 373 K, τ_{cr}(T) is weakly dependent on temperature as G(T), and the athermal τ_G component of τ_{cr} is observed. The ratio τ_{cr}(77 K)/τ_{cr}(300 K) = 2.1. Consequently, the behavior of the initial $Al_{0.3}$CoCrFeNi HEA single crystals is typical of low-strength fcc alloys [23].

Upon reaching a high-strength state at the yield point $\sigma_{0.1}$, $Al_{0.3}$CoCrFeNi HEA single crystals showed features of mechanical behavior that had not previously been manifested in the quenched HEA single crystals. Firstly, in the deformed [1̄44]- and [001]-oriented crystals of the $Al_{0.3}$CoCrFeNi HEA, the τ_{cr} were found to be independent of the crystal orientation at 77 K only, since at the low-temperature deformation, the same stress level of 700 MPa was artificially given, and m_{sl}[1̄44] ≈ m_{sl}[001] [19,20]. At T ≥ 200 K, τ_{cr} became dependent on the crystal orientation, and τ_{cr}[1̄44] > τ_{cr}[001] (Figure 4c).

According to the known models of hardening under the assumption of the additivity of the contributions to τ_{cr} [16,24], the effect of hardening from a defect structure (dislocations, multipoles, twins), $L1_2$ and B2 particles can be determined in the $[\bar{1}44]$-oriented crystals,

$$\tau_{cr} = \tau_{cr}^{Q} + \alpha G b \rho^{1/2} + \delta n G b x^{-1} + \tau_{cr}^{L12} + \tau_{cr}^{B2} \quad (1)$$

and in the [001]-oriented crystals,

$$\tau_{cr} = \tau_{cr}^{Q} + \alpha G b \rho^{1/2} + \tau_{cr}^{L12} + \tau_{cr}^{B2} \quad (2)$$

Here, τ_{cr}^{Q} are the critical shear stresses of the quenched undeformed crystals, which do not depend on the crystal orientation [5,25]; $\Delta\tau_{cr}^{DS} = \alpha G b \rho^{1/2}$ is the hardening caused by dislocations (α is the constant [3], G = 80 GPa [7] is the shear modulus of HEA, b = 0.25 nm is the Burgers vector of the perfect dislocation, ρ is the dislocation density); $\Delta\tau_{cr}^{Tw} = \delta n G b x^{-1}$ is the contribution to hardening from twins (δ is a constant, n = 5–7 is the number of dislocations in a pile up at a tensile strain of 5%, x is the average distance between twin boundaries [26]); and τ_{cr}^{L12} and τ_{cr}^{B2} are the contribution to hardening from $L1_2$ and B2 particles, respectively.

$L1_2$ particles are coherent [15–17], and their effect of hardening is determined by the contribution of the elastic stress fields due to the mismatch between the lattices of the particle and matrix E, and the long-range order in Ni_3Al particles:

$$\Delta\tau_{cr}^{L12}(b) = \Delta\tau_1(b) + \Delta\tau_2(b) \quad (3)$$

where $\Delta\tau_1(b)$ is the contribution of elastic stress fields from the $L1_2$ particles [24],

$$\Delta\tau_1(b) = 3 \cdot G \cdot |E|^{\frac{3}{2}} \cdot \left(\frac{f \cdot r}{b}\right)^{\frac{1}{2}} \quad (4)$$

and $\Delta\tau_2(b)$ is the stress due to ordering in the $L1_2$ particles [16,24],

$$\Delta\tau_2(b) = \frac{\mu}{kb}\left[\left(\frac{4\mu f r}{\pi B}\right)^{\frac{1}{2}} - f\right] \quad (5)$$

Here, E = $\Delta a/a_m$ is the lattice mismatch parameter of the initial matrix, a_m, and $L1_2$ particles, a_p ($\Delta a = a_m - a_p$), r is the particle radius in the slip plane, f is the volume fraction of particles estimated by TEM, b = 0.25 nm is the modulus of the Burgers vector of the a/2 <110> dislocation, μ is the antiphase boundary energy, k is the number of dislocations in the complex and $B = (Gb^2)/2$ is the line tension. The contribution to hardening from $L1_2$ particles, estimated earlier for single crystals of the studied HEA according to Equations (3)–(5), was 18 MPa [17]. Moreover, the $\Delta\tau_{cr}^{L12}$ turned out to be the same for crystals of all orientations, since after the precipitation of $L1_2$ particles, the orientation dependence of CRSS was not observed, and the Schmid law was fulfilled [17].

B2 particles are non-coherent [15,27], and their contribution to hardening, according to [24], can be estimated by the Orowan equation:

$$\tau_{cr}^{B2} = Gb/L \quad (6)$$

Here, L = 250 nm is the average distance between B2 particles. The contribution to hardening from B2 particles, with an average distance between them of L = 250 nm, was 80 MPa according to Equation (6), and turned out to be close to the experimentally obtained data, whereby $\Delta\tau_{cr}^{B2}$ = 60–80 MPa in crystals of both orientations at 77 K. In both orientations, the contribution to the hardening from B2 particles was the same, and remained within the temperature range when studying the temperature dependence of τ_{cr}(T) (Figure 4c). This correlated with the close volume fraction of B2 particles in the crystals of the studied orientations, which was ~20%. The volume fraction of particles was determined

from dark-field images, and 10 pictures from different places on thin foils were used to estimate it. At 77 K in the studied orientations, after ageing, the τ_{cr} values turned out to be close (Figure 4c). In addition, in the $Al_{0.3}$CoCrFeNi HEA single crystals after ageing at 973 K at 50 h, when only B2 particles were precipitated, the τ_{cr} values were not dependent on the crystal orientation in a wide temperature range, as was shown earlier in [27]. All this qualitatively indicates a similar volume fraction of the precipitated B2 particles in the deformed $[\bar{1}44]$- and [001]-oriented crystals. Consequently, in the deformed $[\bar{1}44]$- and [001]-oriented crystals of the $Al_{0.3}$CoCrFeNi HEA, the contribution to the CRSS value from B2 particles, as well as from $L1_2$ particles, does not depend on the crystal orientation.

Thus, the analysis of Equations (1) and (2) and the experimental data presented in Figure 4c shows that the τ_{cr}^{Q}, τ_{cr}^{L12} and τ_{cr}^{B2} in the deformed and aged $Al_{0.3}$CoCrFeNi HEA single crystals are independent of the crystal orientation. Consequently, the orientation dependence of τ_{cr} in the deformed and aged $Al_{0.3}$CoCrFeNi HEA single crystals is due to the orientation dependence of the dislocation structure and, in this case, the dislocation structure with twins makes the largest contribution to the hardening at the yield point, as compared to that without twins. So, $\tau_{cr}^{Q}([\bar{1}44]) = \tau_{cr}^{Q}([001]) = 70$ MPa at 296 K. At 296 K, after low-temperature deformation at 77 K in the [001]-oriented crystals, where there was no twinning, the contribution to hardening at the yield point from the defect structure relative to quenched crystals was $\Delta\tau_{cr} = \Delta\tau_{cr}^{DS} - \tau_{cr}^{Q} = 160$ MPa − 70 MPa = 90 MPa, and in the $[\bar{1}44]$-oriented crystals with twins in the dislocation structure, $\Delta\tau_{cr} = \left(\Delta\tau_{cr}^{DS} + \Delta\tau_{cr}^{Tw}\right) - \tau_{cr}^{Q} = 215$ MPa − 70 MPa = 145 MPa. In the $[\bar{1}44]$-oriented crystals at 296 K, the contribution to hardening at the yield point from the defect structure was 55 MPa greater than in the [001]-oriented crystals (Figure 4c). If we assume that when the stress level of 700 MPa was reached during the low-temperature deformation at 77 K, the contribution of $\Delta\tau_{cr}^{DS} = \alpha G b \rho^{1/2}$ to the $[\bar{1}44]$- and [001]-oriented crystals was similar, then the difference in the stresses $\Delta\tau_{cr}$ in the deformed crystals can be seen to be due to twinning at 296 K. The estimate of the contribution from twins $\tau_{cr}^{Tw} = \delta n G b x^{-1}$ to hardening at the yield point—at an average value of $x = 500$ nm, as determined from TEM data, $\delta = 0.5$ and $n = 5$—was 100 MPa, which correlates quite well with the experimental data.

Moreover, the orientation dependence of the τ_{cr} value of high-strength crystals within a wide temperature range is associated with the different temperature dependence of τ_{cr}(T). In the deformed $[\bar{1}44]$-oriented crystals with twins in the dislocation structure, the τ_S and the temperature dependence of τ_{cr}(T) were weakened (τ_{cr}(77 K)/τ_{cr}(300 K) = 1.3), and τ_{cr}(T) was determined by the temperature dependence of the shear modulus G(T) for the HEAs [7]. In the deformed [001]-oriented crystals without twins in the dislocation structure, as in the initial crystals, the strong temperature dependence of τ_{cr}(T) was preserved (τ_{cr}(77 K)/τ_{cr}(300 K) = 1.7). If, when hardened by plastic deformation, the $\sigma_{0.1}$ in the $[\bar{1}44]$- and [001]-oriented crystals was governed by slip, then the temperature dependence of τ_{cr}(T) should have the same dependence as the initial crystals, and τ_{cr} should not depend on orientation. A weak temperature dependence of τ_{cr}(T), like G(T), was characteristic of twinning from the yield point and its safekeeping over a wide temperature range [28]. A qualitative confirmation of the development of twinning in the deformed $[\bar{1}44]$-oriented crystals from the onset of deformation at T > 200 K is the fact that within a temperature range of 200 to 473 K, the τ_{cr} is close in magnitude to the CRSS for twinning, $\tau_{cr}^{tw} = 200$MPa, obtained with the [011]-oriented crystals of the $Al_{0.3}$CoCrFeNi HEA, with a Schmid factor for twinning, m_{tw}, close to that of $[\bar{1}44]$-orientation ($m_{tw} = 0.47$ in [011]-crystals and $m_{tw} = 0.5$ in $[\bar{1}44]$-orientation) [5].

Secondly, the precipitation of $L1_2$ and B2 particles preserves the orientation dependence of τ_{cr}, induced by low-temperature deformation at 77 K. However, in the deformed $[\bar{1}44]$-crystals after ageing, τ_S and τ_{cr}(T) were again increased. The ratio τ_{cr}(77 K)/τ_{cr}(300 K) = 1.5, and this has been revealed to be close in magnitude to the deformed [001]-crystals, with particles in which the onset of plastic flow was associated with slip and τ_{cr}(77 K)/τ_{cr}(300 K) = 1.7. TEM investigations of the dislocation structure, after strain of 5% at 296 K in the aged $[\bar{1}44]$-crystals, showed that the onset of plastic flow in these crystals was also associated with slip, rather than twinning. Ordered coherent $L1_2$ particles, as was shown earlier in [17], suppress the development of twinning in the $Al_{0.3}$CoCrFeNi HEA single crystals.

Thirdly, in the strain-hardened $[\bar{1}44]$-and [001]-oriented crystals, $\sigma_{0.1}$ and τ_{cr} were found to change only slightly within a temperature range of 573 to 973 K (Figure 4). In polycrystalline CoCrFeMnNi HEA with a grain size of 4.4 μm, $\sigma_{0.1}$ decreased by 1.4 times with an increase in temperature from 673 K to 973 K, due to the GBS, which usually occurs in polycrystals at $T > T_{cr}$ ($T_{cr} = 0.5T_m$ is the critical temperature above which GBS occurs in polycrystals; T_m—melting temperature) (Figure 4b). In strain-hardened $[\bar{1}44]$- and [001]-oriented crystals, there were no grain boundaries, but there were twins and multipoles. Twins are athermal obstacles to moving dislocations, and there is no sliding on them. Multipoles, like twins, are also obstacles to moving dislocations [5]. Both twins and multipoles provide a high stress level at the yield point $\sigma_{0.1}$, and its weak dependence at $T \geq 573$ K. However, the contribution to $\sigma_{0.1}$ from multipoles is smaller than that from twins at $T \geq 573$ K (Figure 4). In the hardened $[\bar{1}44]$- and [001]-oriented crystals with $L1_2$ and B2 particles, the τ_{cr} values change slightly within a temperature range of 573 to 873 K. At $T > 873$ K, τ_{cr} decreases, which can be associated with an increase in the size of B2 particles, and with the partial dissolution of $L1_2$ particles during heating and testing, since the temperature of 873 K is higher than the ageing temperature [15–17], and this requires additional study.

Finally, achieving a high-strength state at the yield point $\sigma_{0.1}$ in the $Al_{0.3}$CoCrFeNi HEA single crystals via deformation and subsequent ageing was accompanied by a decrease in plasticity (3.5–13 times in $[\bar{1}44]$-crystals and 2.3 times in [001]-crystals) (Figure 5), but at the same time, the samples retained their ductile fracture qualities. With an increase in the stress level at the yield point $\sigma_{0.1}$, achieved via the dislocation structure during low-temperature deformation, the uniform strain in the crystals decreased. In the $[\bar{1}44]$-orientation with twins in the dislocation structure, $\sigma_{0.1}$ increased 3–5.5-fold, and the plasticity decreased to 7–13% compared to the initial crystals within a temperature range of 296 to 973 K. In the [001]-oriented crystals without twins in the dislocation structure, $\sigma_{0.1}$ increased 2–4-fold compared to the initial crystals of this orientation, but the plasticity remained equal to 15–20% (Figures 4 and 5).

It should be noted that in the high-strength $[\bar{1}44]$- and [001]- oriented crystals of the $Al_{0.3}$CoCrFeNi HEA under tension at a test temperature of 773 K, a serrated flow was observed on the $\sigma(\varepsilon)$ curves, as in the quenched crystals of this alloy under tension and compression [8,17]. Consequently, in high-strength single crystals of the $Al_{0.3}$CoCrFeNi HEA upon tensile strain at 773 K, dynamic strain ageing was observed, associated with the formation of Cottrell atmospheres by mobile Al atoms near a moving dislocation core [8]. Dynamic strain ageing qualitatively confirms that during the precipitation of particles, some of the Al atoms are in a solid solution and lead to the blocking of moving dislocations. The locking and rapid unlocking of dislocations from the atmosphere of Al atoms leads to a serrated flow on the $\sigma(\varepsilon)$ curves [8,17].

Thus, the achievement of a high-strength state at the yield point $\sigma_{0.1}$ of the $Al_{0.3}$CoCrFeNi HEA single crystals via low-temperature straining and subsequent ageing provides, on the one hand, a high stress level of $\sigma_{0.1}$ at $T > 296$ K and a weak temperature dependence $\sigma_{0.1}(T)$ at high temperatures $T \geq 573$ K, which is determined by the absence of GBS yet, while on the other hand retaining plasticity.

4. Conclusions

It was shown that the achievement of a high-strength state at the yield point $\sigma_{0.1}$ in the $Al_{0.3}$CoCrFeNi HEA single crystals via low-temperature straining at 77 K and ageing at 893 K for 50 h provides a high-stress level of $\sigma_{0.1}$ at $T > 296$ K, and a weak temperature dependence $\sigma_{0.1}(T)$ at high temperatures $T \geq 573$ K, which is determined by the absence of GBS, but at the same time retains plasticity of up to 7–13% in the $[\bar{1}44]$-oriented crystals, and up to 15–20% in the [001]-oriented crystals.

Author Contributions: Conceptualization, I.V.K. and Y.I.C.; methodology, I.V.K. and Y.I.C.; investigation, I.V.K., Z.V.P., A.V.V. and A.A.S.; writing—original draft preparation, I.V.K.; writing—review and editing, I.V.K. and Y.I.C.; funding acquisition, I.V.K. All authors have read and agreed to the published version of the manuscript.

Funding: This research was supported by Russian Science Foundation (project No. 19-19-00217).

Conflicts of Interest: The authors declare no conflict of interest.

References

1. Zhang, Y.; Zuo, T.T.; Tang, Z.; Gao, M.C.; Dahmen, K.A.; Liaw, P.K.; Lu, Z.P. Microstructures and properties of high-entropy alloys. *Prog. Mater. Sci.* **2014**, *61*, 1–93. [CrossRef]
2. Otto, F.; Dlouhy, A.; Somsen, C.; Bei, H.; Eggeler, G.; George, E.P. The influences of temperature and microstructure on the tensile properties of a CoCrFeMnNi high-entropy alloy. *Acta Mater.* **2013**, *61*, 5743–5755. [CrossRef]
3. Laplanche, G.; Kostka, A.; Horst, O.M.; Eggeler, G.; George, E.P. Microstructure evolution and critical stress for twinning in the CrMnFeCoNi high-entropy alloy. *Acta Mater.* **2016**, *118*, 152–163. [CrossRef]
4. Joo, S.-H.; Kato, H.; Jang, M.J.; Moon, J.; Tsai, C.W.; Yeh, J.W.; Kim, H.S. Tensile deformation behavior and deformation twinning of an equimolar CoCrFeMnNi high-entropy alloy. *Mater. Sci. Eng. A* **2017**, *689*, 122–133. [CrossRef]
5. Kireeva, I.V.; Chumlyakov, Y.I.; Pobedennaya, Z.V.; Vyrodova, A.V.; Kuksgauzen, I.V.; Kuksgauzen, D.A. Orientation and temperature dependence of a planar slip and twinning in single crystals of $Al_{0.3}$CoCrFeNi high-entropy alloy. *Mater. Sci. Eng. A* **2018**, *737*, 47–60. [CrossRef]
6. Gludovatz, B.; Hohenwarter, A.; Catoor, D.; Chang, E.H.; George, E.P.; Ritchie, R.O. A fracture-resistant high-entropy alloy for cryogenic applications. *Science* **2014**, *345*, 1153–1158. [CrossRef] [PubMed]
7. Laplanche, G.; Gadaud, P.; Horst, O.; Otto, F.; Eggeler, G.; George, E.P. Temperature dependencies of the elastic moduli and thermal expansion coefficient of an equiatomic single-phase CoCrFeMnNi high-entropy alloy. *J. Alloys Compd.* **2015**, *623*, 348–353. [CrossRef]
8. Yasuda, H.Y.; Shigeno, K.; Nagase, T. Dynamic strain aging of $Al_{0.3}$CoCrFeNi high entropy alloy single crystals. *Scr. Mater.* **2015**, *108*, 80–83. [CrossRef]
9. Yasuda, H.Y.; Miyamoto, H.; Cho, K.; Nagase, T. Formation of ultrafine-grained microstructure in $Al_{0.3}$CoCrFeNi high entropy alloys with grain boundary precipitates. *Mater. Lett.* **2017**, *199*, 120–123. [CrossRef]
10. Li, D.; Li, C.; Feng, T.; Zhang, Y.; Sha, G.; Lewandowski, J.J.; Liaw, P.K.; Zhang, Y. High-entropy $Al_{0.3}$CoCrFeNi alloy fibers with high tensile strength and ductility at ambient and cryogenic temperatures. *Acta Mater.* **2017**, *123*, 285–294. [CrossRef]
11. Li, Z.; Zhao, S.; Diao, H.; Liaw, P.K.; Meyers, M.A. High-velocity deformation of $Al_{0.3}$CoCrFeNi high-entropy alloy: Remarkable resistance to shear failure. *Sci. Rep.* **2017**, *2*, 42742. [CrossRef] [PubMed]
12. Joseph, J.; Stanford, N.; Hodgson, P.; Fabijanic, D.M. Tension/compression asymmetry in additive manufactured face centered cubic high entropy alloy. *Scripta Mater.* **2017**, *129*, 30–34. [CrossRef]
13. Ma, S.C.; Zhang, S.F.; Qiao, J.W.; Wang, Z.H.; Gao, M.C.; Jiao, Z.M.; Yang, H.J.; Zhang, Y. Superior high tensile elongation of a single-crystals CoCrFeNi$Al_{0.3}$ high-entropy alloy by Bridgman solidification. *Intermetallics* **2014**, *54*, 104–109. [CrossRef]
14. Liu, K.; Komarasamy, M.; Gwalani, B.; Shukla, S.; Mishra, R.S. Fatigue behavior of ultrafine grained triplex $Al_{0.3}$CoCrFeNi high entropy alloy. *Scr. Mater.* **2019**, *158*, 116–120. [CrossRef]
15. Gwalani, B.; Soni, V.; Lee, M.; Mantri, S.A.; Ren, Y.; Banerjee, R. Optimizing the coupled effects of Hall-Petch and precipitation strengthening in a $Al_{0.3}$CoCrFeNi high entropy alloy. *Mater. Des.* **2017**, *121*, 254–260. [CrossRef]
16. He, J.Y.; Wang, H.; Huang, H.L.; Xu, X.D.; Chen, M.W.; Wu, Y.; Liu, X.J.; Nieh, T.G.; An, K.; Lu, Z.P. A precipitation-hardened high-entropy alloy with outstanding tensile properties. *Acta Mater.* **2016**, *102*, 187–196. [CrossRef]
17. Kireeva, I.V.; Chumlyakov, Y.I.; Pobedennaya, Z.V.; Vyrodova, A.V. Effect of γ′-phase particles on the orientation and temperature dependence of the mechanical behaviour of $Al_{0.3}$CoCrFeNi high entropy alloy single crystals. *Mater. Sci. Eng. A* **2020**, *772*, 138772. [CrossRef]
18. Choudhuri, D.; Shukla, S.; Gwalani, B.; Banerjee, R.; Mishra, R.S. Deformation induced intermediate metastable lattice structures facilitate ordered B2 nucleation in fcc-based high entropy alloy. *Mater. Res. Lett.* **2019**, *7*, 40–46. [CrossRef]
19. Abuzaid, W.; Sehitoglu, H. Critical resolved shear stress for slip and twin nucleation in single crystalline FeNiCoCrMn high entropy alloy. *Mater. Charact.* **2017**, *129*, 288–299. [CrossRef]
20. Bönisch, M.; Wu, Y.; Sehitoglu, H. Hardening by slip-twin and twin-twin interactions in FeMnNiCoCr. *Acta Mater.* **2018**, *153*, 391–403. [CrossRef]

21. Kireeva, I.V.; Chumlyakov, Y.I.; Vyrodova, A.V.; Pobedennaya, Z.V.; Karaman, I. Effect of twinning on the orientation dependence of mechanical behavior and fracture in single crystals of the equiatomic CoCrFeMnNi high-entropy alloy at 77K. *Mater. Sci. Eng. A* **2020**, *784*, 139315. [CrossRef]
22. Barrett, C.S.; Massalski, T.B. *Structure of Metals: Crystallographic Methods, Principles, and Data, Pergamon*; Pergamon: New York, NY, USA, 1980; 654p.
23. Honeycombe, R.W.K. *The Plastic Deformation of Metals*, 2nd ed.; Edward Arnold: London, UK, 1984; 483p.
24. Nembach, E. *Particle Strengthening of Metals and Alloys*; John Wiley & Sons, Inc.: New York, NY, USA, 1997; 285p.
25. Kireeva, I.V.; Chumlyakov, Y.I.; Pobedennaya, Z.V.; Vyrodova, A.V.; Kuksgauzen, I.V.; Poklonov, V.V.; Kuksgauzen, D.A. The orientation dependence of critical shear stresses in $Al_{0.3}$CoCrFeNi high-entropy alloy single crystals. *Thech. Phys. Lett.* **2017**, *43*, 615–618. [CrossRef]
26. Remy, L. The interaction between slip and twinning systems and the influence of twinning on the mechanical behavior of fcc materials and alloys. *Metall. Trans. A* **1981**, *12*, 387–408. [CrossRef]
27. Kireeva, I.V.; Chumlyakov, Y.I.; Pobedennaya, Z.V.; Vyrodova, A.V.; Saraeva, A.A.; Bessonova, I.G.; Kuksgauzen, I.V.; Kuksgauzen, D.A. Temperature and orientation dependence of the mechanical properties of $Al_{0.3}$CoCrFeNi high-entropy alloy single crystals hardened by non-coherent β-phase particles. *Russ. Phys. J.* **2020**, *63*, 134–141. [CrossRef]
28. Chumlyakov, Y.I.; Kireeva, I.V.; Korotaev, A.D.; Litvinova, E.I.; Zuev, Y.L. Mechanisms of the plastic deformation, hardening and fracture in single crystals of nitrogen-containing austenitic stainless steel. *Russ. Phys. J.* **1996**, *39*, 189–210. [CrossRef]